Monte Carlo dosimetry for ^{125}I and ^{103}Pd eye plaque brachytherapy with various seed models

R. M. Thomson[a] and D. W. O. Rogers
Ottawa Carleton Institute for Physics, Carleton University Campus, Ottawa, Ontario K1S 5B6, Canada

(Received 4 August 2009; revised 23 October 2009; accepted for publication 10 November 2009; published 23 December 2009)

Purpose: Dose distributions are calculated for various models of ^{125}I and ^{103}Pd seeds in the standardized plaques of the Collaborative Ocular Melanoma Study (COMS). The sensitivity to seed model of dose distributions and dose distributions relative to TG-43 are investigated.
Methods: Monte Carlo simulations are carried out with the EGSnrc user-code BrachyDose. Brachytherapy seeds and eye plaques are fully modeled. Simulations of one seed in the central slot of a 20 mm Modulay (gold alloy) plaque backing with and without the Silastic (silicone polymer) insert and of a 16 mm fully loaded Modulay/Silastic plaque are performed. Dose distributions are compared to those calculated under TG-43 assumptions, i.e., ignoring the effects of the plaque backing and insert and interseed attenuation. Three-dimensional dose distributions for different ^{125}I and ^{103}Pd seed models are compared via depth-dose curves, isodose contours, and tabulation of doses at points of interest in the eye. Results are compared to those of our recent BrachyDose study for COMS plaques containing model 6711 (^{125}I) or 200 (^{103}Pd) seeds [R. M. Thomson *et al.*, Med. Phys. **35**, 5530–5543 (2008)].
Results: Along the central axis of a plaque containing one seed, variations of less than 1% are seen in the effect of the Modulay backing alone for different seed models; for the Modulay/Silastic combination, variations are 2%. For a 16 mm plaque fully loaded with ^{125}I (^{103}Pd) seeds, dose decreases relative to TG-43 doses are 11%–12% (19%–20%) and 14%–15% (20%) at distances of 0.5 and 1 cm from the inner sclera along the plaque's central axis, respectively. For the same prescription dose, doses at points of interest vary by up to 8% with seed model. Doses to critical normal structures are lower for all ^{103}Pd seed models than for ^{125}I with the possible exception of the sclera adjacent to the plaque; scleral doses vary with seed model and are not always higher for ^{103}Pd than for ^{125}I.
Conclusions: Dose decreases relative to doses calculated under TG-43 assumptions vary slightly with seed model (for each radionuclide). Dose distributions are sensitive to seed model; however, variations are generally no larger than the magnitudes of other systematic uncertainties in eye plaque therapy.
[DOI: 10.1118/1.3271104]

Key words: eye plaque, COMS, choroidal melanoma, BrachyDose, Monte Carlo, dose calculation, brachytherapy, EGSnrc

I. INTRODUCTION

Choroidal melanoma is the most common primary intraocular malignancy. Therapeutic interventions for this cancer were evaluated in the Collaborative Ocular Melanoma Study (COMS), initiated in the mid-1980s. In 2001, the COMS group reported that survival rates for enucleation (removal of the eye) and ^{125}I eye plaque brachytherapy were the same,[1] and this was later confirmed in 2006.[2] Plaques of a standardized design[3] were used for COMS, consisting of a Modulay (gold alloy) backing containing a Silastic (silicone polymer) seed carrier. COMS plaques continue to be widely used for eye plaque therapy.

The protocol described by Task Group 43 (TG-43) of the American Association of Physicists in Medicine (AAPM)[4,5] is widely used for treatment planning for eye plaque therapy.[6] In this approach, inhomogeneities in the seeds' vicinity (plaque backing, insert, air, etc.) are ignored and dose to water is calculated. Taking into account the Modulay backing and Silastic insert and seed-to-seed interactions, dose decreases relative to TG-43 calculations are 14% for ^{125}I (Oncura/GE/Amersham Health Oncoseed 6711) and 20% for ^{103}Pd (Theragenics TheraSeed 200) at 1 cm from the inner sclera on the central axis of COMS plaques.[7,8] Doses to critical normal structures in the eye can differ by 30% or more compared to TG-43 calculations.[7] Dose reductions of up to 10% result from replacing a portion of the water phantom with air.[7,9] Delivered doses thus differ significantly from those calculated under the TG-43 protocol.

Recent Monte Carlo studies[7,8] of dosimetry for eye plaque therapy have focused on model 6711 and 200 seeds for ^{125}I and ^{103}Pd, respectively; however, other seed models are used for eye plaque therapy. In addition to these two seed models, six other seeds with adequate air kerma strength for eye plaque therapy have been identified (Table I). Seed models differ through the shape and thickness of encapsulation, the

TABLE I. Brachytherapy sources simulated. Trade names and the average energy of photons emitted from seeds are those quoted by Usher-Moga *et al.* (Ref. 10); the average energy is not available for the model IAPd-103 seed. The extent of (radio)activity (distance along a seed's longitudinal axis between the two extremities of radioactive material) is estimated using the descriptions of Taylor and Rogers (Refs. 19 and 20).

Radioisotope	Manufacturer	Model	Trade name	Average energy (keV)	Activity extent (mm)
^{125}I	Oncura/GE/Amersham Health	6711	Oncoseed	27.34	2.8
	Best Medical International	2301	Best I-125 Source	28.50	4.0
	International Brachytherapy Co.	1251L	InterSource125	28.50	3.7
	Implant Sciences Corporation	3500	I-Plant I-125	28.15	3.8
	IsoAid	IAI-125	Advantage I-125	27.33	3.0
^{103}Pd	Theragenics Corporation	200	TheraSeed	20.71	3.3
	Best Medical International	2335	Best Pd-103 Source	20.71	4.8
	IsoAid	IAPd-103	Advantage Pd-103	···	3.6

distribution of radioactive material within the encapsulation, the type of radiographic marker, and materials.[10] Physical characteristics of photons emitted by different seed models (position, energy, location, and direction) are strongly dependent on seed construction, especially since brachytherapy sources are often constructed of high atomic number materials.[11] These characteristics affect interactions in the plaque's Modulay backing and Silastic insert,[7] as well as seed-to-seed interactions.[12] Thus, differences in seed models will be reflected in dose distributions for eye plaque therapy.

In this work, the sensitivity of dose distributions to seed model for eye plaque therapy using COMS plaques is studied using Monte Carlo methods. The seed models considered are those listed in Table I. Given the state of flux of seed models on the market, this is likely not an exhaustive list of seeds which may be used for eye plaque therapy; however, it should be adequate to illustrate differences between seed models. The effects of the Modulay backing alone and the Modulay backing and Silastic insert combination on doses are compared for a single seed of each model. Three-dimensional dose distributions for a fully loaded COMS 16 mm plaque are calculated in the eye region for each seed model. Dose distributions are compared to those calculated under TG-43 assumptions to ascertain whether differences relative to TG-43 vary with seed model. Dose distributions are compared via depth-dose curves, isodose contours, and tabulation of doses at points of interest.

II. METHODS

Simulations are performed with the EGSnrc (Refs. 13 and 14) user-code BrachyDose.[15,16] Simulation details (e.g., dose scoring, physics processes simulated, and plaque descriptions including composition of Modulay and Silastic) are described in our BrachyDose study of COMS plaques containing models 6711 (^{125}I) and 200 (^{103}Pd) seeds.[7] As such, many details are omitted from this section.

The COMS 20 mm plaque with a single seed in its central slot and the COMS 16 mm plaque fully loaded with 13 seeds are both simulated. Plaques are modeled at the center of a $(30\ \text{cm})^3$ water phantom of mass density $0.998\ \text{g/cm}^3$; 10^{11} histories are simulated and dose is scored in $(0.05\ \text{cm})^3$ voxels. Simulations of the fully loaded 16 mm plaque are compared to simulations performed under TG-43 assumptions, herein referred to as "TG-43-sim," with the same configuration of seeds in water and no interseed interactions, plaque backing, or insert.[7,17]

The seed models used in this study (Table I) were previously benchmarked[18,19] and dosimetry parameters for each seed model appear in the Carleton Laboratory for Radiotherapy Physics TG-43 Database.[20] Table I lists the average energy of photons emitted from seeds of each model, as reported by Usher-Moga *et al.*,[10] based on measurements of the seeds' spectroscopic output with a high-purity germanium detector. Due to the fluorescence x rays from silver (22, 25 keV), the average energy of photons emitted from ^{125}I seed models containing silver (6711, 3500, and IAI-125) is slightly lower than for seed models without silver (2301 and 1251L). The average energy of photons emitted (above 5 keV) for a bare ^{125}I (^{103}Pd) source is 28.37 keV (20.74 keV).[5]

In Table I, the extent of radioactivity in the brachytherapy sources is the distance along a seed's longitudinal axis between the two extremities of radioactive material. For example, the extent of radioactivity is the cylinder length for cylindrical sources and the distance between the outer edges of the outermost beads for bead sources. In some cases, this length coincides with the "active length" defined by TG-43U1.[5]

The eye (X,Y,Z) and plaque (x,y,z) coordinate frames were described previously.[7,17] The origin of the eye reference frame (X,Y,Z) is at the center of the eye (Fig. 1). The eye is idealized as a sphere of diameter 2.46 cm with a sclera 0.1 cm thick. The plaque reference frame (x,y,z) has its origin at the inner sclera (0.1 cm inset from the concave side of the Silastic insert) on the plaque's central axis. The z axis coincides with the plaque's central axis.

Doses are tabulated at eight points of interest in the eye region (Fig. 1) for a right eye: sclera adjacent to the plaque,

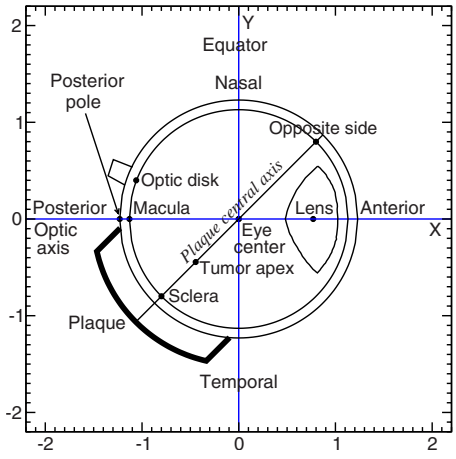

FIG. 1. Configuration for eye plaque therapy (scale in centimeters). The X and Y axes in the eye reference frame are shown. The origin of the plaque coordinate system coincides with the scleral dose point, marked "Sclera." As an example, a plaque midway between the posterior pole and equator temporal is shown. All points of interest, with the exception of the lacrimal gland (which does not lie in the plane shown), are indicated.

tumor apex, eye center, opposite side of the eye to the plaque, macula, center of the lens, optic disk, and lacrimal gland. The exact positions of these points are given by Thomson *et al.*,[7] [except for the lacrimal gland at $(X,Y,Z)=(0.77,-0.82,0.82)$ cm] and coincide with the coordinates of the points of interest being used by Task Group 129 of the AAPM for dosimetric comparisons.[22]

As the plaque is simulated at the center of a water phantom with no air interface, the symmetries of the configuration mean that doses at certain points (e.g., the plaque's central axis) are the same for different plaque positions. Doses at off-axis points of interest depend on plaque placement. To approximate many different possible plaque placements in the eye, eight different plaque positions are considered: Four plaques centered on the equator (temporal, nasal, superior, and inferior) and, similarly, four between the equator and posterior pole. For conciseness, doses at off-axis points of interest are only explicitly reported in Sec. III for a few plaque positions: Plaques centered on the equator (temporal and nasal) and positioned midway between the equator and posterior pole (inferior and superior.) Doses at the lens and macula are the same for the plaques on the equator and, separately, for the plaques midway between the equator and posterior pole.

Results are quoted with 1σ statistical uncertainties. These uncertainties are at most 0.03% on the dose at the prescription point (tumor apex) D_{Rx}, and 0.1% (0.2%) or less at the other points of interest for ^{125}I (^{103}Pd) seeds. Nonstatistical uncertainties outweigh statistical uncertainties. In addition to uncertainties discussed previously,[7] the following sources of uncertainty are relevant for the current work: The coordinates of seed centers are assumed to be the same for all seed models and seeds in a Silastic insert are modeled as completely surrounded by Silastic. In reality, seeds are inserted in slots in a Silastic carrier. Air gaps may exist about seeds and the size of these gaps may vary with seed design. If Silastic inserts with seed slots of the same size and in the same positions are used for treatments with different seed models, then the seed center coordinates will not be the same for all seeds as seed diameters vary. The 6711, 2301, IAI-125, 2335, and IAPd-103 models all have outer diameters of 0.800 mm, while the 1251L, 3500, and 200 models have outer diameters of 0.810, 0.836, and 0.826 mm, respectively. However, if the Silastic insert is customized for each seed diameter, seed center coordinates will remain the same for treatments with different seed models. The components within brachytherapy seeds may move and the magnitude of displacements will vary with seed model. These considerations will likely have little effect on ratios of doses reported here.

Simulation times vary slightly with seed model. For example, simulations of 10^{10} histories (which give 0.1% uncertainty on the dose at the tumor apex D_{Rx}) for a 16 mm plaque while scoring in $(0.05\ \text{cm})^3$ voxels take 25–36 h (17–21 h) for ^{125}I (^{103}Pd) seed models (using a particle recycling feature to enhance efficiency[7]). For clinical applications, simulation times would be substantially shorter because such small statistical uncertainties are not required. Simulations achieving 2% (1%) uncertainty on the dose at the tumor apex in $(0.05\ \text{cm})^3$ voxels take less than 3 minutes (12 minutes).

III. RESULTS AND DISCUSSION

III.A. Effect of the Modulay backing

The effect of the plaque backing alone on the central axis dose for a single seed is shown in Fig. 2 for different seed models. For all seed models, there is a small dose enhancement near the plaque (small z), followed by a significant dose decrease. Near the plaque, differences of 0.5% or less between seed models are evident. For ^{125}I (^{103}Pd) seeds, dose decreases are 10%–11% (6%–6.3%) at the opposite side of the eye to the plaque.

The high Z materials of the plaque backing enhance photoelectric absorption and decrease Compton scatter relative to water.[7,21] Dose enhancements near the plaque are due to the emission of fluorescence photons from the plaque backing. The spectrum of fluorescent photons depends on the spectrum of photons emitted by the brachytherapy seed, and hence varies with seed model. The differences shown in Fig. 2 between seed models of the same radionuclide are related to the average energy of photons emitted from each seed (Table I). The higher average energy of photons from model 2301 and 1251L seeds (28.50 keV) means that more fluorescence photons and photons of slightly higher average energy are emitted from the plaque backing for these models than for the other seeds, resulting in the largest dose enhancements. Dose enhancements are smaller for model 3500 seeds (28.15 keV), and even smaller for model 6711 (27.34 keV) and IAI-125 (27.33 keV) seeds.

III.B. Effect of the Modulay backing and Silastic insert

Dose decreases (relative to TG-43 conditions) along the central axis due to the Modulay backing and Silastic insert for a single seed are shown in Fig. 3 for each seed model.

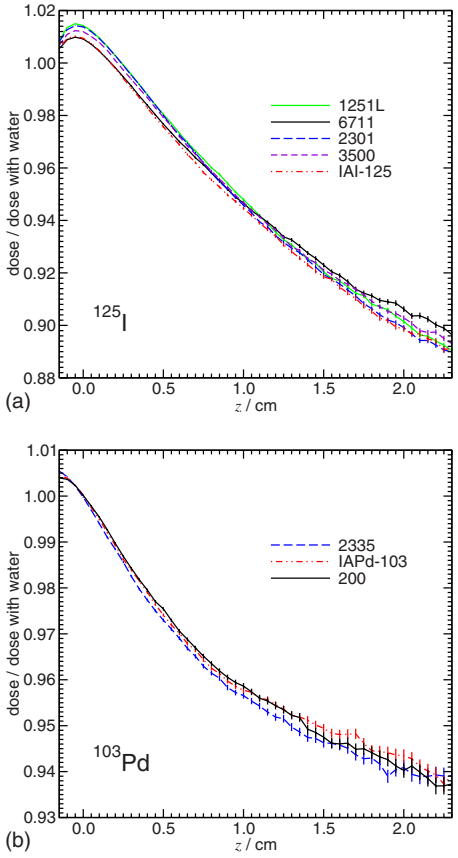

FIG. 2. Ratio of the doses along the plaque's central axis for a single seed in a 20 mm COMS plaque backing (no Silastic insert) to the doses for the same seed in water (no backing or insert) for different models of (a) ^{125}I and (b) ^{103}Pd seeds.

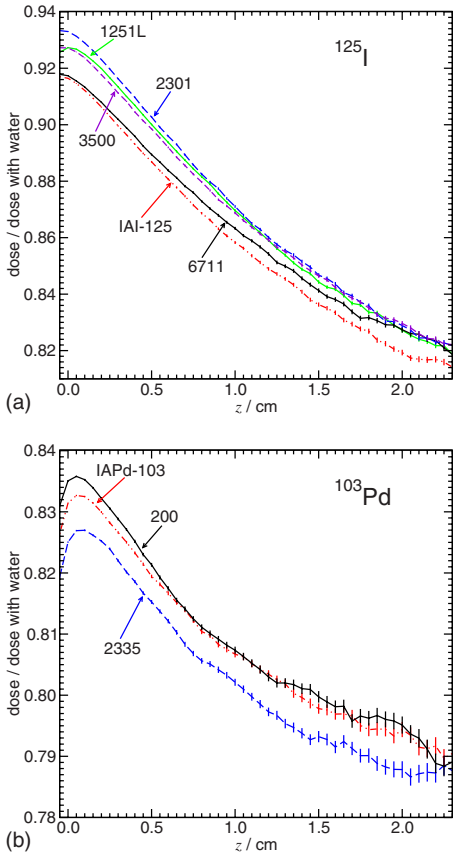

FIG. 3. Ratio of the doses along the plaque's central axis for a single seed in a 20 mm COMS (Modulay/Silastic) plaque to the doses for the same seed in water (no backing or insert) for different models of (a) ^{125}I and (b) ^{103}Pd seeds.

The inclusion of the Silastic insert further reduces doses and changes dose profiles. Relative dose decreases differ by up to nearly 2% for ^{125}I seeds, with dose decreases being largest for model IAI-125 seeds and smallest for 2301. For ^{103}Pd seeds, dose decreases are slightly larger for 2335 and IAPd-103 seeds than for the model 200 seeds previously studied.[7] Dose reductions near the plaque (small z) are 7%–8% (17%–18%) for ^{125}I (^{103}Pd) seeds. At the opposite side of the eye to the plaque, the dose is reduced by 18% (21%) for ^{125}I (^{103}Pd) seeds.

Variations in the relative effect of the plaque backing and insert for seed models of the same radionuclide are due to differences in source geometry and materials. Emitted photon spectra vary with seed model, resulting in slightly different average cross sections for interactions in Modulay and Silastic. The shape and size of radioactive sources within the plaque differ with seed model, even though the coordinates of seed centers are identical for all seed models. The effect of the Modulay backing alone was roughly the same for 6711 and IAI-125 seeds near the plaque; however, the effect of the Modulay/Silastic combination is not the same for the two models. The extent of radioactivity (Table I) for the 6711 seed is 2.8 mm versus 3.0 mm for IAI-125, both spread evenly over these lengths. Due to the concave nature of the Silastic insert, photons from the IAI-125 seed must, on average, travel through more Silastic to exit the plaque than those from the 6711 seed. As Silastic is a more attenuating medium than water,[7,21] this results in more attenuation of photons from the IAI-125 seed than from 6711, and hence a slightly larger dose decrease. The relative effect of the backing alone was also roughly the same for 2301 and 1251L seeds, but is not the same for the Modulay/Silastic combination. The distribution of activity is different for these two seed models. While the 2301 source consists of a single cylinder 4.0 mm long, the 1251L source consists of one central annulus 0.5 mm long separated by 0.8 mm from two 0.8 mm long outer annuli. Photons from the 1251L source must, on average, travel through more Silastic than those from the 2301 source to reach points near the plaque on the central axis (small z). This results in the larger dose decreases seen in Fig. 3 for the 1251L seed than for the 2301 seed. For the ^{103}Pd seeds, the dose decrease is most important for the 2335 seed (4.8 mm) and least important for the 200 seed (3.3 mm), with the IAPd-103 seed (3.6 mm) between the other two.

Each curve in Fig. 3(b) has roughly the same shape, with curves increasing slightly with z before decreasing. As explained previously,[7] this is due to the source geometries of each ^{103}Pd seed in which the radioactive sources are separated by a marker at the seed center. With no radioactivity at the seed center, photons travel through more Silastic to reach

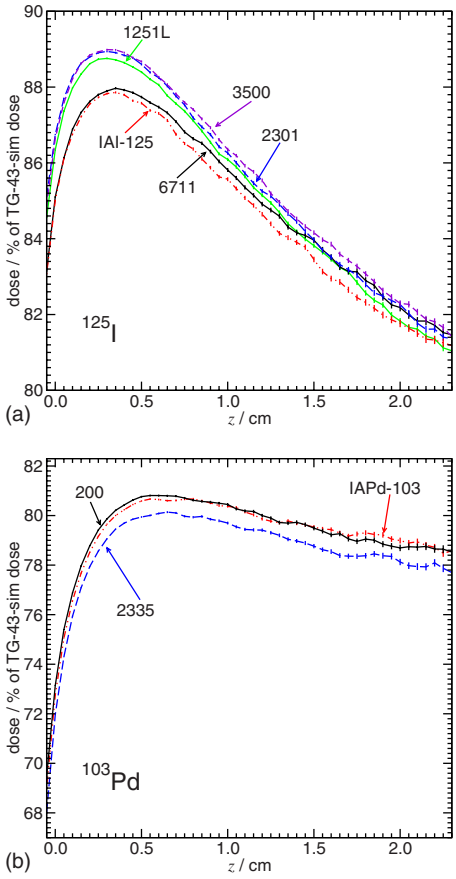

FIG. 4. Central axis depth dose curves for seeds in a 16 mm COMS plaque for (a) ^{125}I and (b) ^{103}Pd seeds. Doses are quoted relative to the doses for TG-43-sim, i.e., doses for the same seeds in water with no interseed interactions.

areas very near the insert on the central axis than to reach areas slightly further out. Silastic is a more attenuating medium than water,[7,21] and hence fewer photons reach the small z region when the insert is present. This results in the increasing dose ratio for small z.

III.C. Multiseed configurations: COMS 16 mm plaque

Based on simulations of the 16 mm fully loaded Modulay/Silastic plaque with and without interseed effects, doses along the plaque's central axis are decreased by less than 1% due to interseed attenuation. For ^{125}I seed models, interseed attenuation is slightly larger for the 2301 and 1251L models (at a little more than 0.5%) than for the other three models (less than 0.5%). For the three models of ^{103}Pd seeds, interseed attenuation is roughly the same and is less than 0.5%. Omitting the Modulay backing and Silastic insert (seeds in water), interseed attenuation results in dose decreases of less than 2%.

Doses along the central axis of the fully loaded 16 mm plaque are presented in Fig. 4 as percentages of TG-43-sim doses, i.e., the doses for the same seeds in water with no interseed interactions. For all seed models, dose decreases near the plaque (small z) are larger than those for the single seed (Fig. 3). Photons from off-axis seeds must travel through more Silastic to reach the small z scoring region than those from a central seed, resulting in more attenuation in Silastic and higher dose decreases in this region.[7]

The shapes of curves for different seed models of the same radionuclide are similar. For ^{125}I seeds, dose reductions relative to TG-43-sim vary by up to 2% near the plaque ($z<1$ cm). Dose reductions in this region are more important for the 6711 and IAI-125 seeds models than for the 1251L, 2301, and 3500 models, as in Fig. 3 (discussed previously). At the sclera, dose reductions are 15% for the 6711 and IAI-125 models versus 14% for 1251L and 13% for 2301 and 3500 (Table II). At the tumor apex (z=0.5 cm), dose reductions vary by a bit more than 1%. Further along the central axis ($z>1$ cm), dose reductions are nearly the same for all ^{125}I seed models, and are 18%–19% at the opposite side of the eye. For ^{103}Pd models, dose decreases are 27%–28% at the sclera, and vary by 1% at the tumor apex and at the opposite side of the eye from the plaque.

TABLE II. Doses at points of interest as percentages of TG-43-sim doses for a 16 mm fully loaded COMS plaque. Doses at off-axis points are for plaques centered on the equator. The statistical uncertainty on each entry is at most ±0.2.

Plaque position	Point of interest	^{125}I					^{103}Pd		
		6711	2301	1251L	3500	IAI-125	200	2335	IAPd-103
Any	Sclera	85.1	86.7	86.3	86.6	85.0	73.1	72.0	72.8
	Apex	87.7	88.6	88.4	88.7	87.6	80.8	79.9	80.6
	Center of eye	85.2	85.6	85.5	85.8	85.0	80.2	79.4	80.1
	Opposite side	81.5	81.4	81.1	81.6	81.2	78.6	77.8	78.5
Equator	Macula	77.8	77.8	77.6	78.0	77.4	71.0	69.8	71.0
	Lens	82.1	82.3	82.2	82.4	81.9	76.4	75.5	76.4
Equator temporal	Optic disk	79.3	79.2	79.0	79.4	79.0	74.3	73.3	74.4
	Lacrimal gland	16.9	16.9	17.0	17.2	16.3	12.3	11.2	12.3
Equator nasal	Optic disk	74.8	75.4	74.2	74.4	74.5	65.0	63.9	65.5
	Lacrimal gland	78.9	78.5	78.4	78.8	78.5	74.9	73.7	74.8

TABLE III. Doses in gray at points of interest for ^{103}Pd seeds for TG-43-sim and simulations of the COMS 16 mm plaque. Doses at off-axis points are for plaques centered on the equator. Statistical uncertainties are at most 0.2%. The air kerma strength per seed needed to obtain a dose of 85 Gy at the prescription point (5 mm from the inner sclera on the plaque's central axis) for seeds in water with no interseed interactions (i.e., TG-43-sim) in 168 h is used for each seed model (1 U=1 μGy m^2 h^{-1}).

Plaque position	Point of interest	TG-43-sim			16 mm COMS plaque		
		200	2335	IAPd-103	200	2335	IAPd-103
Any	Sclera	288	268	281	211	193	204
	Apex	85.0	85.0	85.0	68.7	67.9	68.5
	Eye center	22.8	23.6	23.3	18.3	18.7	18.7
	Opposite side	3.74	3.99	3.91	2.94	3.11	3.07
Equator	Macula	11.4	12.1	11.8	8.09	8.44	8.37
	Lens	16.4	17.1	16.9	12.5	12.9	12.9
Equator temporal	Optic disk	7.17	7.54	7.41	5.32	5.53	5.51
	Lacrimal gland	32.3	36.1	33.6	3.97	4.05	4.12
Equator nasal	Optic disk	21.7	23.1	22.2	14.1	14.8	14.5
	Lacrimal gland	4.04	4.22	4.14	3.03	3.11	3.10
S_K (U/seed)		4.04	4.28	4.09	4.04	4.28	4.09

As expected from the previous study with models 6711 (^{125}I) and 200 (^{103}Pd) seeds,[7] dose decreases relative to TG-43-sim doses at off-axis points of interest vary considerably with plaque position. Variations in dose decreases relative to TG-43-sim doses between seed models of the same radionuclide are not nearly as significant. For example, with ^{125}I (^{103}Pd) seeds, doses at the lacrimal gland are 16%–17% (11%–12%) and 78%–79% (74%–75%) of the TG-43-sim doses for plaques on the equator temporal and nasal, respectively (Table II). Dose decreases of between 11% and 89% relative to TG-43-sim doses are seen at the points of interest. For each plaque configuration and point of interest listed in Table II (i.e., each row), the absolute (not percent) difference between entries for any two seeds of the same radionuclide is generally less than 2%. This is generally true for all eight plaque positions considered. The percent difference between entries (in Table II) varies with the magnitude of dose decrease.

Table III displays doses in gray at points of interest for the 16 mm plaque on the equator temporal and nasal for ^{103}Pd seeds for TG-43-sim and full simulations. The air kerma strength used for each seed model is that needed to deliver 85 Gy to the tumor apex in 168 h for seeds in water with no interseed interactions. TG-43-sim doses differ by up to 11% at the points of interest for the different seed models, with differences of 7% at the sclera, 6% at the macula, and 11% at the lacrimal gland for the plaque on the equator temporal. Taking into account the plaque backing, insert, and interseed interactions, doses are reduced substantially, as expected. Of particular note is the dose decrease at the lacrimal gland for the plaque on the equator temporal: From 32–36 to 4 Gy. Doses at the prescription point decrease from 85 to 67.9–68.7 Gy. Doses at the sclera differ by up to 9% for different seed models. At other points of interest, doses generally vary by 5% or less with seed model. Table IV lists analogous doses for ^{125}I seeds in plaques positioned midway between the equator and posterior pole superior and inferior. Doses vary by up to 10% with seed model.

Doses at points of interest for the 16 mm plaque are presented in Table V as percentages of the dose at the prescription point, D_{Rx}. Doses at the sclera range from 279% to 299% of D_{Rx} for ^{125}I seeds, with the highest doses for the 6711 and IAI-125 models. For ^{103}Pd seeds, scleral doses range from 284% to 307% of D_{Rx}, with the highest dose for model 200 seeds. Hence, (absolute) scleral doses vary by up to 8% for seed models of each radionuclide. Apart from the sclera, dose differences of 1%–2% of D_{Rx} are seen at points of interest in the eye for seed models of the same radionuclide. Doses at the center of the eye range from 32% to 33% of D_{Rx} for ^{125}I and are lower at about 27%–28% of D_{Rx} for ^{103}Pd models, amounting to variations of up to 4% in the local dose.

For the same prescription dose, doses at points of interest are consistently lower for all ^{103}Pd seed models than for ^{125}I seed models, with the possible exception of the sclera. The scleral dose is highest for model 200 ^{103}Pd seeds at 307% of D_{Rx}, followed by 299% of D_{Rx} for model 6711 seeds. Scleral doses for the other ^{103}Pd seeds (284% and 298% for 2335 and IAPd-103, respectively) fall within the range of 279%–299% of scleral doses for ^{125}I seeds.

Figure 5(a) displays isodose contours for the two models of Best seeds: 2301 (^{125}I) and 2335 (^{103}Pd). Requiring the same prescription dose, the scleral dose is nearly the same for both of these seeds. However, dose distributions differ considerably, with doses decreasing more rapidly for ^{103}Pd seeds. The 5% isodose line lies within the eye for the ^{103}Pd

TABLE IV. Doses in gray at points of interest for ^{125}I seeds for TG-43-sim and simulations of the COMS 16 mm plaque. Doses at off-axis points are given for plaques midway between the equator and the posterior pole ("Eq. and p.p."). Statistical uncertainties are at most 0.1%. The air kerma strength per seed to obtain a dose of 85 Gy at the prescription point (5 mm from the inner sclera on the plaque's central axis) for seeds in water with no interseed interactions (i.e., TG-43-sim) in 100 h is used for each seed model (1 U=1 μGy m^2 h^{-1}).

Plaque position	Point of interest	TG-43-sim					16 mm COMS plaque				
		6711	2301	1251L	3500	IAI-125	6711	2301	1251L	3500	IAI-125
Any	Sclera	262	247	243	250	261	223	214	210	217	222
	Apex	85.0	85.0	85.0	85.0	85.0	74.6	75.3	75.1	75.4	74.4
	Eye center	28.0	29.2	29.2	28.8	28.0	23.9	25.0	25.0	24.8	23.8
	Opposite side	6.86	7.54	7.55	7.34	6.87	5.59	6.14	6.12	5.99	5.58
Eq. and p.p.	Macula	74.4	75.5	74.9	74.2	77.1	59.1	61.0	60.3	59.9	61.2
	Lens	12.3	13.1	13.1	12.8	12.6	10.1	10.8	10.8	10.6	10.3
Eq. and p.p. superior	Optic disk	60.6	62.2	62.3	60.9	64.2	47.0	49.0	48.9	47.8	49.6
	Lacrimal gland	13.6	14.5	14.5	14.0	14.1	9.08	9.62	9.58	9.43	9.4
Eq. and p.p. inferior	Optic disk	60.6	62.2	62.3	60.9	64.2	47.0	49.0	48.9	47.8	49.6
	Lacrimal gland	6.09	6.69	6.69	6.50	6.21	4.88	5.32	5.32	5.19	4.93
S_K (U/seed)		4.76	4.50	4.67	4.50	4.78	4.76	4.50	4.67	4.50	4.78

seeds, but not for the ^{125}I seeds. Figure 5(b) is the analogous plot for the IsoAid Advantage seeds. Note that the 5% isodose contour for IAI-125 seeds is visible in Fig. 5(b).

IV. CONCLUSIONS

Dose decreases relative to doses calculated under TG-43 assumptions are sensitive to seed model (for each radionuclide). However, these decreases are close to those for model 6711 (^{125}I) and 200 (^{103}Pd) seeds, studied previously.[7] Along the central axis of a plaque containing a single seed, differences of less than 1% in the effect of the Modulay backing alone and 2% in the effect of the Modulay and Silastic combination are seen between seed models of the same radionuclide. Interseed attenuation results in small dose decreases in the eye region, as seen for model 6711 (^{125}I) and 200 (^{103}Pd) seeds,[7] and these vary only slightly with seed model. For a fully loaded COMS 16 mm plaque, decreases relative to TG-43-sim doses are 11%–12% (19%–20%) and 14%–15% (20%) at distances of 0.5 and 1 cm, respectively, from the inner sclera on the plaque's central axis. At points of interest in the eye, dose decreases relative to TG-43-sim vary with seed model by about the same amount as along the central axis; with doses expressed as percentages of TG-43-sim doses, absolute (not percent) differences are generally less than 2% between seed models of the same radionuclide.

Requiring the same prescription dose (at 0.5 cm from the inner sclera on the plaque's central axis), dose distributions are sensitive to seed model. Doses calculated under TG-43 assumptions differ by up to 11% for different seed models of the same radionuclide. Full simulations of the COMS 16 mm

TABLE V. Doses at points of interest as percentages of the dose at the prescription point (the tumor apex, at z=0.5 cm on the plaque's central axis) D_{Rx} for seeds in a fully loaded COMS 16 mm plaque. Statistical uncertainties are at most 0.1% of D_{Rx}.

Plaque position	Point of interest	^{125}I					^{103}Pd		
		6711	2301	1251L	3500	IAI-125	200	2335	IAPd-103
Any	Sclera	299	285	279	288	298	307	284	298
	Eye center	32.0	33.2	33.2	32.8	32.0	26.6	27.6	27.2
	Opposite side	7.49	8.15	8.14	7.95	7.49	4.29	4.57	4.48
Equator	Macula	17.2	18.1	18.1	17.6	17.7	11.8	12.4	12.2
	Lens	24.0	24.9	24.9	24.4	24.7	18.3	19.0	18.9
Equator temporal	Optic disk	12.1	12.8	12.8	12.5	12.4	7.76	8.14	8.05
	Lacrimal gland	9.03	9.47	9.49	9.30	9.35	5.79	5.96	6.01
Equator nasal	Optic disk	27.8	29.2	28.7	28.0	28.8	20.5	21.7	21.2
	Lacrimal gland	7.68	8.21	8.23	8.00	7.87	4.42	4.57	4.52

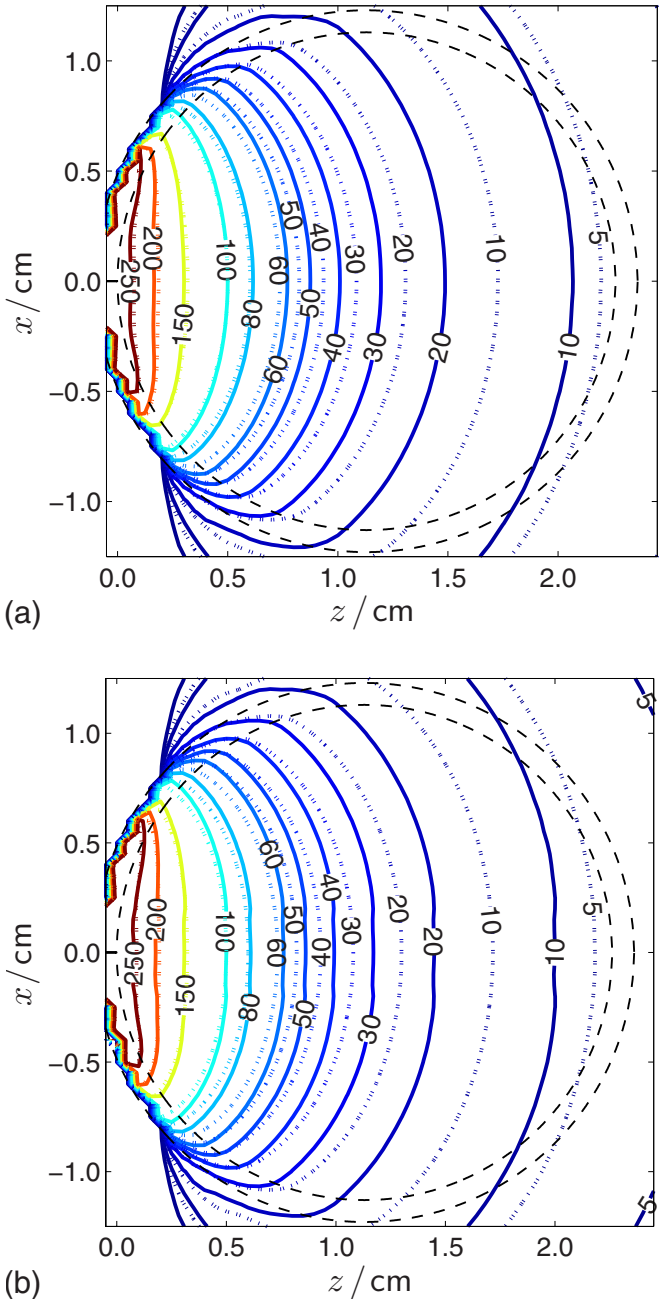

FIG. 5. Isodose contours in the xz plane ($y=0$) for the COMS 16 mm plaque containing model (a) 2301 ^{125}I (solid lines) or 2335 ^{103}Pd (dotted lines) and (b) IAI-125 ^{125}I (solid lines) or IAPd-103 ^{103}Pd (dotted lines) seeds. Dose is 100% at the prescription point. Dashed circles indicate the outlines of the eye and inner sclera. The plaque is simulated at the center of a water phantom. Dose is set to zero in voxels intersecting the plaque.

plaque indicate that scleral dose variation with seed model is fairly significant at 20% (23%) of D_{Rx} for ^{125}I (^{103}Pd) seed models. For a prescription dose of the order of 70 Gy, scleral doses can differ by 14 Gy or more. However, as scleral doses are large, the largest percent difference in scleral doses for two seed models of the same radionuclide is 8%. At other points of interest further from the plaque, doses generally vary by a few percent of D_{Rx} for seed models of the same radionuclide, amounting to differences of order 1 Gy.

Doses at points of interest are lower (for the eight plaque positions considered) for all ^{103}Pd seed models than for ^{125}I models, with the possible exception of the sclera. This is consistent with previous results for the 6711 (^{125}I) and 200 (^{103}Pd) seed models.[7] Scleral doses vary with seed model. The previous BrachyDose study showed that the scleral dose for model 200 ^{103}Pd seeds was 3% higher than for model 6711 ^{125}I seeds.[7] Scleral doses are not consistently higher for ^{103}Pd seed models than for ^{125}I; rather, scleral doses for the other models of ^{103}Pd seeds considered (2335 and IAPd-103) fall within the range of doses for ^{125}I seed models.

The current clinical significance of variations in dose distributions with seed model can be assessed by considering the magnitude of systematic uncertainties for eye plaque therapy. For these treatments, the position of the plaque relative to ocular structures is only known approximately. Dosimetric uncertainties depend on the local dose gradient. A 0.5 mm shift in the position of the prescription point results in a 10% change in dose; a 1 mm shift at the opposite side of the eye to the plaque changes dose by less than 1% of D_{Rx}. Further, the nominal uncertainty on source strength is 2%. Hence, dose variations with seed model (for each radionuclide) are generally no larger than the magnitudes of other systematic uncertainties in eye plaque therapy.

Toward improving eye plaque dose calculations, corrections accounting for heterogeneities (plaque backing and insert; interseed effects) may be applied to TG-43 calculations. The results of the current study suggest that, as a first step, heterogeneity corrections derived for model 6711 (^{125}I) and 200 (^{103}Pd) seeds may be used for other models of ^{125}I and ^{103}Pd seeds, respectively. In the longer term, it is hoped that full Monte Carlo simulations may be used for dose calculations. BrachyDose simulation times are sufficiently fast for clinical applications for all seed models considered.

ACKNOWLEDGMENTS

This work was supported by the Natural Sciences and Engineering Research Council of Canada, the Canada Research Chairs program, the Canada Foundation for Innovation, the Ontario Innovation Trust, the office of the Vice President of Research at Carleton University, and the Ministry of Research and Innovation of Ontario. The authors would like to thank Sou-Tung Chiu-Tsao for her careful reading of the manuscript.

[a]Electronic mail: rthomson@physics.carleton.ca

[1]COMS Group, "The COMS randomized trial of iodine 125 brachytherapy for choroidal melanoma. III. Initial mortality findings. COMS report no. 18," Arch. Ophthalmol. (Chicago) **105**, 969–982 (2001).
[2]COMS Group, "The COMS randomized trial of iodine 125 brachytherapy for choroidal melanom. V. Twelve-year mortality rates and prognostic factors: COMS report no. 28," Arch. Ophthalmol. (Chicago) **124**, 1684–1693 (2006).
[3]R. W. Kline and P. D. Yeakel, "Ocular melanoma, I-125 plaques," Med. Phys. **14**, 475 (Abs) (1987).
[4]R. Nath, L. L. Anderson, G. Luxton, K. A. Weaver, J. F. Williamson, and A. S. Meigooni, "Dosimetry of interstitial brachytherapy sources: Recommendations of the AAPM Radiation Therapy Committee Task Group No. 43," Med. Phys. **22**, 209–234 (1995).
[5]M. J. Rivard, B. M. Coursey, L. A. DeWerd, M. S. Huq, G. S. Ibbott, M. G. Mitch, R. Nath, and J. F. Williamson, "Update of AAPM Task Group No. 43 Report: A revised AAPM protocol for brachytherapy dose calcu-

lations," Med. Phys. **31**, 633–674 (2004).
[6]COMS Group, Ch 12: Radiation Therapy, COMS Manual of Procedures PB95–179693, Springfield, VA, National Technical Information Service (1995), 1999 Revision at http://www.jhu.edu/wctb/coms/manual/coms_chap12.pdf, accessed October 15, 2009.
[7]R. M. Thomson, R. E. P. Taylor, and D. W. O. Rogers, "Monte Carlo dosimetry for ^{125}I and ^{103}Pd eye plaque brachytherapy," Med. Phys. **35**, 5530–5543 (2008).
[8]C. S. Melhus and M. J. Rivard, "COMS eye plaque brachytherapy dosimetry simulations for ^{103}Pd, ^{125}I, and ^{131}Cs," Med. Phys. **35**, 3364–3371 (2008).
[9]A. de la Zerda, S. Chiu-Tsao, J. Lin, L. L. Boulay, I. Kanna, J. H. Kim, and H. Tsao, "^{125}I plaque dose distribution including penumbra characteristics," Med. Phys. **23**, 407–418 (1996).
[10]J. Usher-Moga, S. M. Beach, and L. A. DeWerd, "Spectroscopic output of ^{125}I and ^{103}Pd low dose rate brachytherapy sources," Med. Phys. **36**, 270–278 (2009).
[11]R. Nath and Z. J. Chen, "Silver fluorescent x-ray yield and its influence on the dose rate constant for nine low-energy brachytherapy source models," Med. Phys. **34**, 3785–3793 (2007).
[12]H. Afsharpour, M. D'Amours, B. Coté, J.-F. Carrier, F. Verhaegen, and L. Beaulieu, "A Monte Carlo study on the effect of seed design on the interseed attenuation in permanent prostate implants," Med. Phys. **35**, 3671–3681 (2008).
[13]I. Kawrakow and D. W. O. Rogers, "The EGSnrc code system: Monte Carlo simulation of electron and photon transport," Technical Report No. PIRS–701, National Research Council of Canada, Ottawa, Canada, 2000.
[14]I. Kawrakow, "Accurate condensed history Monte Carlo simulation of electron transport. I. EGSnrc, the new EGS4 version," Med. Phys. **27**, 485–498 (2000).
[15]G. Yegin and D. W. O. Rogers, "A fast Monte Carlo code for multi-seed brachytherapy treatments including interseed effects," Med. Phys. **31**, 1771 (Abs) (2004).
[16]G. Yegin, R. E. P. Taylor, and D. W. O. Rogers, "BrachyDose: A new fast Monte Carlo code for brachytherapy calculations," Med. Phys. **33**, 2074 (Abs) (2006).
[17]R. M. Thomson, K. M. Furutani, J. S. Pulido, S. L. Stafford, and D. W. O. Rogers, "Modified COMS plaques for ^{125}I and ^{103}Pd iris melanoma brachytherapy," Int. J. Radiat. Oncol., Biol., Phys. (in press).
[18]R. E. P. Taylor, G. Yegin, and D. W. O. Rogers, "Benchmarking BrachyDose: Voxel-based EGSnrc Monte Carlo calculations of TG–43 dosimetry parameters," Med. Phys. **34**, 445–457 (2007).
[19]R. E. P. Taylor and D. W. O. Rogers, "An EGSnrc Monte Carlo-calculated database of TG-43 parameters," Med. Phys. **35**, 4228–4241 (2008).
[20]R. E. P. Taylor and D. W. O. Rogers, The Carleton Laboratory for Radiotherapy Physics TG-43 Parameter Database, http://www.physics.carleton.ca/clrp/seed_database.
[21]M. A. Astrahan, "Improved treatment planning for COMS eye plaques," Int. J. Radiat. Oncol., Biol., Phys. **61**, 1227–1242 (2005).
[22]S. Chiu-Tsao, personal communication (2009).